ISSN: 0067-2904

Preparation and Study Some Properties of Ferrite Nanoparticles ($Cu_xAl_{0.3-x}Ni_{0.7}Fe_2O_4$)

Shaimaa A. Kadhim, Tagreed M. Al- Saadi*
College of Education for Pure Science/Ibn Al- Haitham, University of Baghdad, Baghdad, Iraq

Received: 7/11/2022 Accepted: 18/6/2023 Published: 30/7/2024

Abstract:

The current study includes the preparation of $Cu_xAl_{0.3-x}Ni_{0.7}Fe_2O_4$ ferrite nanoparticles where: x = 0, 0.05, 0.1, 0.15, 0.2, 0.25, and 0.3 using the auto combustion method (sol-gel). The citric acid was used as fuel for auto combustion. The X-ray diffraction (XRD) test showed an increase in the crystal lattice constant, which is of face-centered cubic (FCC) structure. Field Emission Scanning Electron Microscopy (FE-SEM) showed that the compound has apparent porosity; its grains are spherical or semi-spherical and within the nanoscale. The Energy-Dispersive X-ray spectroscopy (EDX) proved the presence of all the elements involved in the preparation of the compound, and there are no other elements, which means that it is of high purity. The vibrating sample magnetometer (VSM) showed that the hysteresis loop is small and narrow, meaning the wasted energy is as little as possible. In addition, it was found that the compound has good sensitivity to NO_2 gas.

Keywords: ferrite nanoparticles, structural properties, magnetic properties, NO_2 gas, sensitivity.

تحضير ودراسة بعض خصائص جسيمات الفرايت النانوية ($Cu_xAl_{0.3-x}Ni_{0.7}Fe_2O_4$)

شيماء كاظم ، تغريد مسلم

كلية التربية للعلوم الصرفة/ابن الهيثم، جامعة بغداد، بغداد، العراق

الخلاصة

تتضمن الدراسة الحالية تحضير جسيمات الفرايت النانوية $Cu_xAl_{0.3-x}Ni_{0.7}Fe_2O_4$ باستخدام طريقة الاحتراق التلقائي (sol–gel) حيث ان : x= 0 ، 0.05 ، 0.1 ، 0.15 ، 0.2 ، 0.25 ، 0.3 وتم استخدام حامض الستريك كوقود للاحتراق الذاتي . أظهرت نتائج اختبار حيود الأشعة السينية (XRD) أن هناك زيادة في ثابت الشبيكة البلورية، وهو يمتلك تركيب مكعب متمركز الوجه(FCC) . أظهر فحص المجهر الإلكتروني الماسح –الباعث للمجال (FE–SEM) أن المركب له مسامية واضحة وأن حبيباته كروية أو شبه كروية وضمن المقياس النانوي. أما عن التحليل الطيفي للأشعة السينية المشتتة للطاقة (EDX) فقد أثبت وجود جميع العناصر التي تدخل في تحضير المركب، ولا توجد عناصر أخرى مما يعني أنه عالي النقاوة. أظهر مقياس المغناطيسية للعينة الاهتزازية (VSM) أن حلقة الهسترة صغيرة وضيقة، مما يعني أن الطاقة المهدورة تكون قليلة قدر الإمكان. من ناحية أخرى، وجد أن المركب لديه حساسية جيدة لغاز NO_2.

*Email: Shaimaa.Ahmed1104a@ihcoedu.uobaghdad.edu.iq

1. Introduction

Recent technological and industrial advances result in increased hazardous gas emissions that damage internal spaces. Some of these gases are quite toxic; even a concentration of a few tens of ppm poses a risk to human life. As a result, monitoring and controlling the quality of the environment requires very sensitive and selective gas detectors [1]. A conductometric gas sensor is a device that identifies gaseous species in an environment by measuring electrical resistance changes [2, 3]. This sort of sensor is intriguing for usage in portable field applications because of its multiple advantages, which include its simple manufacturing procedure, small size, and ease of use [1].

Spinel ferrites (with a general structural formula of MFe_2O_4) have been used as substitute materials in the gas sensor industry. The fluctuation of the spinel ferrites electrical, acoustic, optical, or calorimetric characteristics provides the basis for gas sensor detection. Detection based on electrical property variability is generating the most attention because it is easy, quick, and of low cost. Due to the growing demand for sensors in smart devices for remote sensing, electrical detection-based sensors are being developed more quickly because of portability and operating system compatibility [3, 4]. It has been observed that MFe_2O_4 spinel ferrites oxides are sensitive substances to oxidizing and reducing gases [5]. Nano ferrites have attracted the attention of researchers due to their easily changeable features and their wide range of possible uses in sensors, microwave devices, magnetic recording, adsorbents, and data storage [6]. For the cation site in the spinel ferrite structure of gas sensors, hundreds of metal oxide materials as thick or extremely thin films are placed as active layers. The 32 oxygen atoms that make up the spinel structure are arranged in a cubic crystal system with 64 tetrahedral sites. 32-site octahedral gas sensors are helpful for chemical control, home security, and environmental monitoring. More innovative materials are being developed for high-performance solid-state gas sensors [7]. Researchers have looked at the use of many unique semiconductor oxides in thin-film forms, thick films, and bulk ceramics as sensing elements in gas sensors [6]. Fe-Fe interactions affect the structural, electrical, and magnetic properties of ferrite, as the presence of impurity ions in the spinel structure gives strong magnetic and electrical properties to ferrite [8]. It has been reported that ferrite modified with rare earth ions distorts the structure of spinel, induces stress, and significantly alters magnetic properties [9, 10]. Because of the confined nature of 4f electrons, the rare earth elements exhibit a strong magneto-crystalline anisotropy, extremely high magnetostriction at low temperatures, and high magnetic moments. As a result, doping with a small quantity of rare earth ions can lead to advancements in the magnetic characteristics of nano-ferrites, particularly the magnetic coercive, making the ferrite suitable for usage in many applications [8].

In this article $Cu_xAl_{0.3-X}Ni_{0.7}Fe_2O_4$ spinel ferrite nanoparticles with different molar concentration of Cu and Al ions, such that x = 0, 0.05, 0.1, 0.15, 0.2, 0.25, and 0.3 were prepared by auto combustion (sol-gel) method. The structural and magnetic properties were studied; also its sensitivity characteristics to NO_2 gas was investigated.

2. Experimental

The auto combustion (sol-gel) method was used to prepare $Cu_xAl_{0.3-X}Ni_{0.7}Fe_2O_4$ nanoparticles where x = 0, 0.05, 0.1, 0.15, 0.2, 0.25, and 0.3. The proportions of the raw materials were fixed as follows: nickel nitrate at N = 0.7, m = 8.14268 g, iron nitrate n = 2, m = 32.32g, citric acid n= 3, with a mass of 23.0556 g, and the rest of the experimental materials as shown in Table 1.

Table 1: Masses of the raw materials used in the preparation of ferrite nanoparticles samples $Cu_xAl_{0.3-X}Ni_{0.7}Fe_2O_4$ and their molar ratios

aluminum nitrate		copper nitrate	
$n_{0.3-x}$	m(g)	n_x	m(g)
0.3	4.50156	0	0
0.25	3.7513	0.05	0.4832
0.2	3.00104	0.1	0.9664
0.15	2.25078	0.15	1.4496
0.1	1.50052	0.2	1.9328
0.05	0.75026	0.25	2.416
0	0	0.3	2.8992

The metal nitrate was placed in a 1000 ml heat-resistant beaker to which 40 mL of deionized water was added. In a different beaker, 40 mL of purified deionized water was added to citric acid, which was mixed with the nitrate solution. The two solutions were mixed well without heating using a magnetic stirrer to obtain a homogeneous solution. Ammonia was added dropwise to the mixture until the pH was equalized to (7). The magnetic mixer heater was turned on until the temperature of the mixture reached 90 °C. The mixing process continued with heating until the mixture turned into a gel. Then the mixer motor was stopped while heating continued until the gel ignited automatically and completely. The resulting ferrite was left to cool and then ground using a ceramic mortar. The ferrite powder was prepared with different molar concentrations of copper ions (x = 0, 0.05, 0.1, 0.15, 0.2, 0.25, and 0.3). The ferrite powder for each molar concentration (the different samples) was put in an oven at 600° C for two hours. XRD, FE-SEM, EDX, and VSM techniques were employed to study the structural and magnetic properties of the prepared ferrite powder samples. After making the mentioned measurements, (1.5 grams) of powder from each sample was pressed manually with a piston under 200 bar pressure for one minute to obtain discs of 1cm diameter and 3.5 mm thickness. The samples were sintered in an oven at 900°C for two hours. Seven samples of $Cu_xAl_{0.3-X}Ni_{0.7}Fe_2O_4$ nanoparticles were prepared, then electrodes were made for all samples, and the sensitivity of each sample to NO_2 gas was measured by a gas sensitivity system.

3. Results and Discussion

3.1. Structural Test

The X-ray diffraction patterns of $Cu_xAl_{0.3-X}Ni_{0.7}Fe_2O_4$ ferrite nanoparticles samples are shown in Figure (1), which were compared with the diffraction pattern with JCPDS standard card no. 10-0325 for $NiFe_2O_4$. Seven peaks within the range (20º-80º) belonging to the planes (111), (220), (311), (400), (422), (511), (440) were noticed from the prepared samples patterns. The peaks indicate the nature of the crystal structure of the ferrite powder of the prepared compound, which was a face-centered cubic spinel-type (FCC) [10].

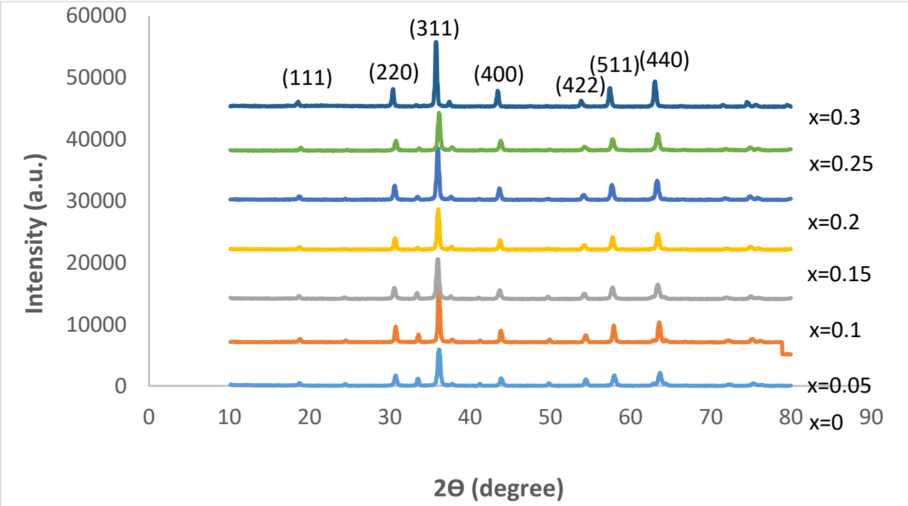

Figure 1: The X-ray diffraction patterns of $Cu_xAl_{0.3-x}Ni_{0.7}Fe_2O_4$ ferrite nanoparticles samples. The lattice parameters were calculated by "Fullprof suit software" and the crystallite size was calculated by Scherrer equation [11, 12]:

$$D_{Sh} = K\lambda / \beta \cos\theta \quad \ldots\ldots (1)$$

Where: λ is the wavelength of the X-ray (1.54 Å), β is the full width at half maximum, K is the shape factor and θ is the incident angle. These values are shown in Table (2).

Table 2: Lattice constants (lattice constant, crystallite size and density)

Cu Content (mole)	Lattice constant (Å)	Crystallite size (nm)	Density (g/cm^3)
0	8.29027	34.30	5.398
0.05	8.30641	31.90	5.367
0.1	8.31565	34.30	5.349
0.15	8.32698	29.80	5.327
0.2	8.33509	35.28	5.311
0.25	8.35207	26.41	5.279
0.3	8.35432	33.21	5.275

From the table, it can be noted that the lattice constant increases with the increase of the molar concentrations of copper ions (x = 0, 0.05, 0.1, 0.15, 0.2, 0.25, and 0.3). Due to the migration of iron cations Fe^{3+} from the tetrahedral spaces to the octahedral to be replaced by impurity cations and the resulting expansion of the tetrahedral spaces, the addition of Cu and Al ions and their increased ratio raised the value of the lattice constant [13]. This change in the lattice constant value is especially important in nanocrystals, where the ratio of the surface area of the nanocrystal to its size is large [14]. The change in the lattice constant indicates that the alternative ions have entered the crystal system in a substitution or interstitial manner between the iron ions; this resulted in the lattice expanding. In addition, a decrease in the density value can be noticed to decrease with the increase of the Cu content [15].

3.2. SEM and EDX Analysis

The Field Emission Scanning Electron Microscope (FE-SEM) technique was used to photograph the samples of the prepared compound ($Cu_xAl_{0.3-x}Ni_{0.7}Fe_2O_4$) (Figure 2) to accurately identify the nature of the surface and shape of the particles and their rate of grain size. From these images, it is clear that the grains are actually within the nanometer range. In addition, the nanoparticles of the samples are spherical or semi-spherical in shape, with some

gatherings or agglomerations. There are also spaces between the agglomerations regions, and these voids represent the porous nature of the surface of the compound, which is necessary for gas adsorption [16]. The reason for the presence of pores is the increase in the value of the crystal lattice constant due to the addition of Cu and Al ions, which leads to an increase in the specific surface area relative to the volume of the compound. This porous structure increases the response of the sensor made of the prepared compound to the gas used for testing [17].

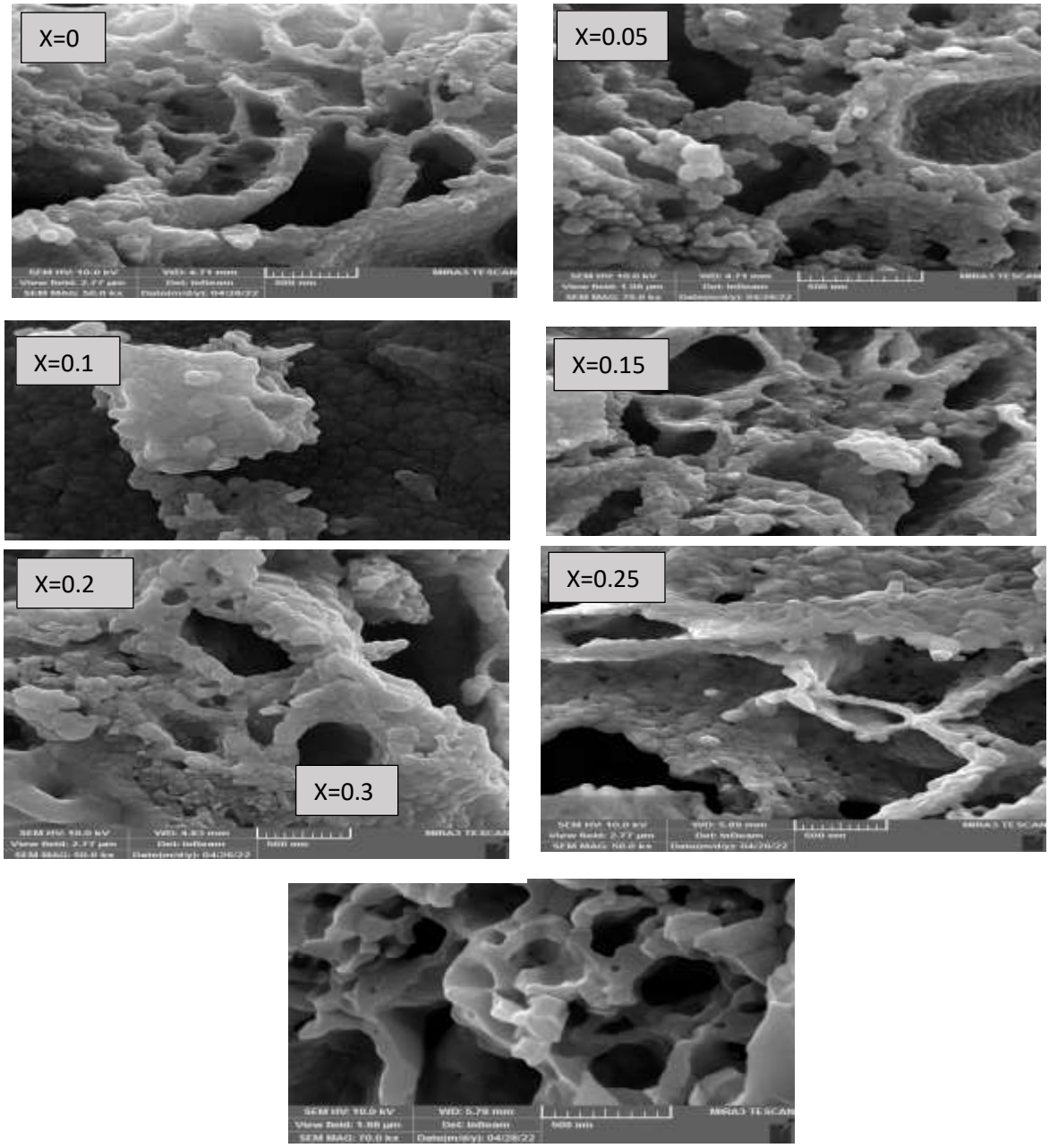

Figure 2: FE-SEM images of the $Cu_xAl_{0.3-x}Ni_{0.7}Fe_2O_4$ ferrite nanoparticles samples.

As for the Energy Dispersive X-ray spectroscopy (EDX) was attached to the emitting field scanning electron microscope (FE-SEM) to detect the presence of the constituent elements of the compound ($Cu_xAl_{0.3-x}Ni_{0.7}Fe_2O_4$), as shown in Figure (3).

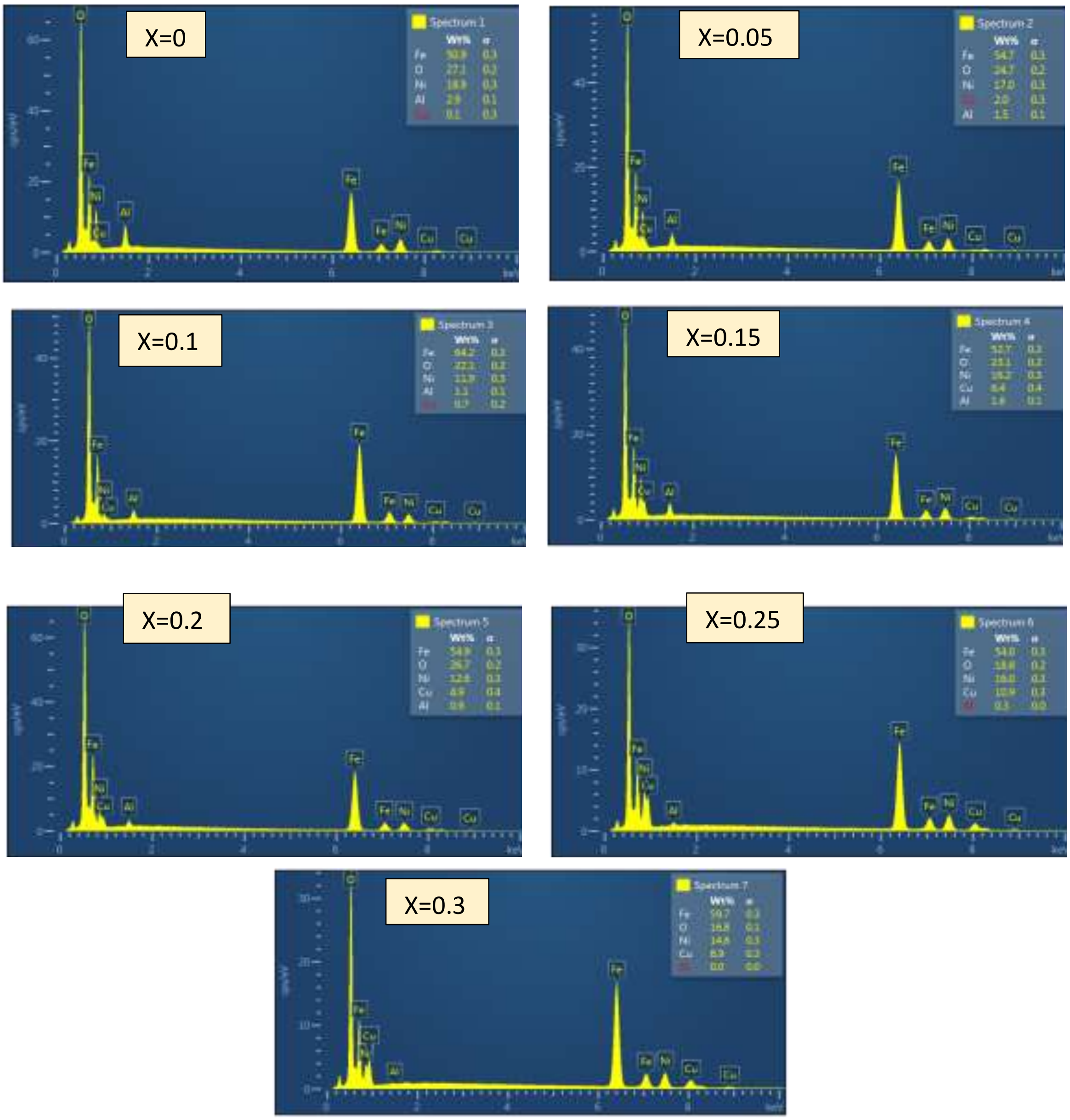

Figure 3: EDX images of the ferrite nanoparticles samples $Cu_xAl_{0.3-x}Ni_{0.7}Fe_2O_4$

3.3. Sensing properties:

The sensitivity of the $Cu_xAl_{0.3-x}Ni_{0.7}Fe_2O_4$ samples to nitrogen dioxide gas (NO_2) was calculated using Equation (2) at different operating temperatures [18]:

$$S = (|Ra - Rg|/Ra)*100\% \quad \ldots\ldots (2)$$

Where: Ra is the sensor sample's electrical resistance in air, Rg is the gas-sensitive sample's electrical resistance. The results showed that the sensitivity to NO_2 changes with the change in operating temperature, as shown in Figure (4).

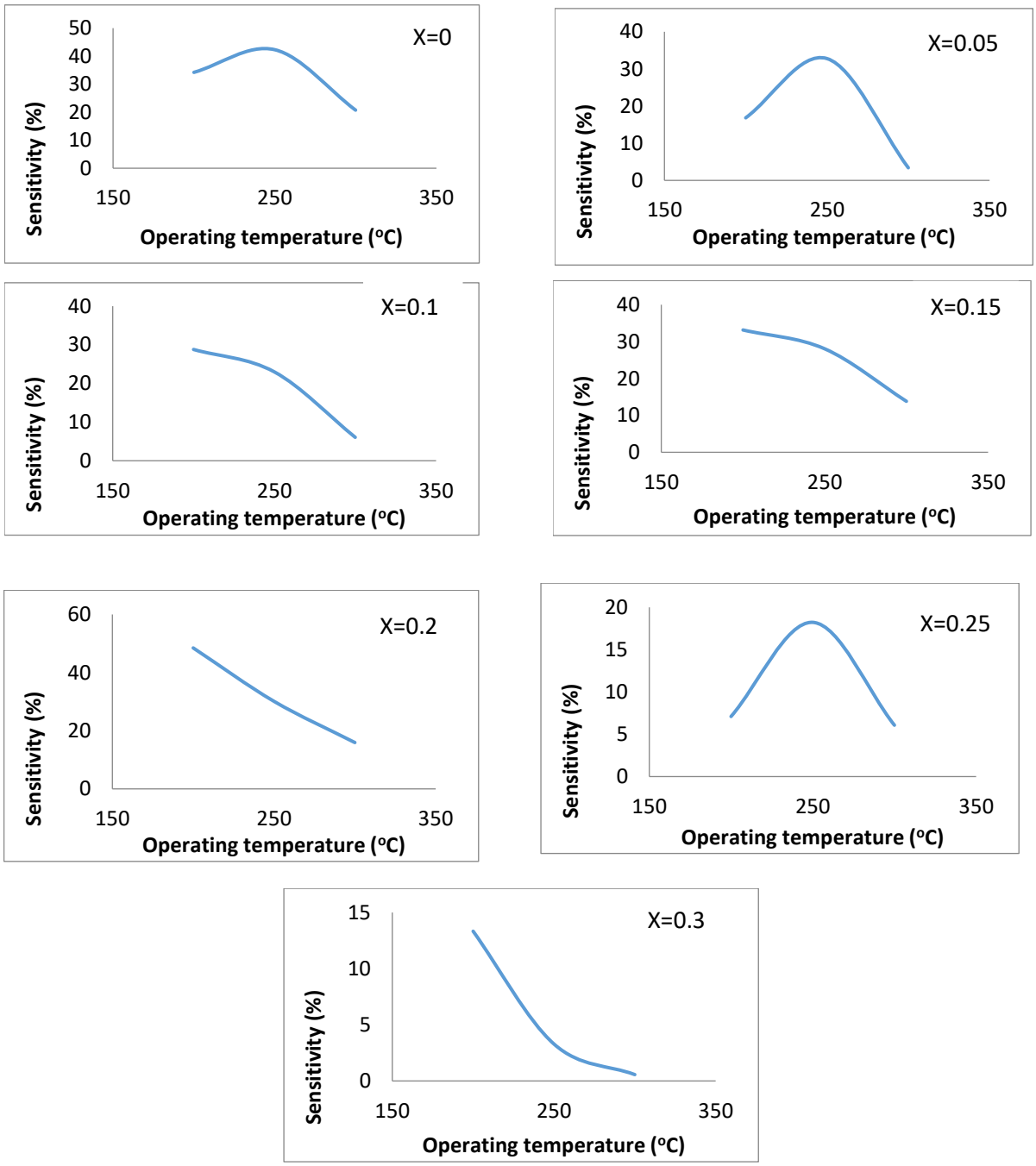

Figure 4: The sensitivity of the $Cu_xAl_{0.3-x}Ni_{0.7}Fe_2O_4$ samples to the operating temperature.

Table (3) shows the highest sensitivity values of the prepared compound samples, and it is noted that the highest sensitivity value was at 200 ºC when Cu content was 0.20 mole.

Table3: The highest sensitivity values of $Cu_xAl_{0.3-x}Ni_{0.7}Fe_2O_4$ nanoparticles samples to the NO_2 gas at different operating temperatures.

Cu Content (mole)	Operating temperature (℃)	Highest sensitivity value (%)
0.05	250	32.78846154
0.1	200	28.79581152
0.15	200	33.15429688
0.2	200	48.48901099
0.25	250	18.22429907
0.3	200	13.33333333

The sensitivity of the $Cu_xAl_{0.3-x}Ni_{0.7}Fe_2O_4$ samples was tested to nitrogen dioxide (NO_2) gas, which is of the oxidizing type. The samples showed an acceptable response to the above gas, which allows its use in some applications. For oxidizing gases, the voltage barrier between the surfaces of molecules is large, and this leads to the formation of resistance to the movement of negative charge carriers(electrons) greater than that to reducing gases [19]. The results show that the activation process of the ferrite nanoparticles $NiFe_2O_4$ increased the value of the crystal lattice constant, which led to a porous structure that increased the specific surface area of the compound, which in turn increased the sensitivity of the sensor to the test gas [20].

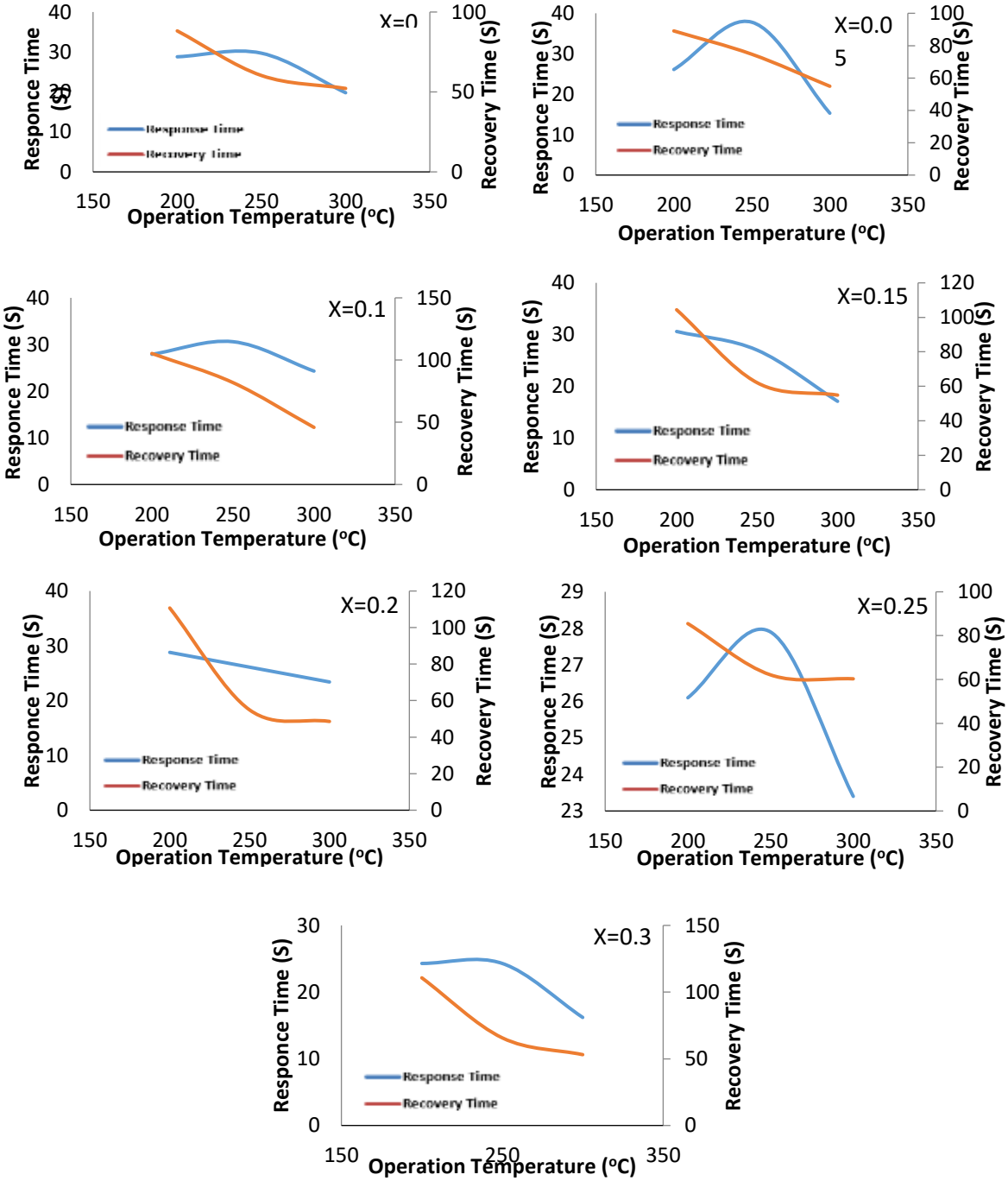

Figure 5: The response time and recovery time of NO_2 gas at different operating temperatures for ferrite nanoparticles $Cu_xAl_{0.3-x}Ni_{0.7}Fe_2O_4$.

Figure (5) shows that both the response and recovery times depend on the Cu and Al content, which are in specific proportions for each added ion. The lattice constant changed with the change of the Cu and Al content (as seen in Table 2), which affects the surface area of the compound and therefore affects both the response time and the recovery time [21]. The response time and recovery time also depend on the geometric shape of the columns or electrodes, and they depend on the speed of the interaction between the oxygen atoms in the atmosphere and the gas atoms to be detected. The response and recovery times depend on the granular surface porosity of the sensor material and operating temperature as an external factor [22]. The sample is selected for appropriate use according to response and recovery time.

The graphs of Figure (5) show that the minimum response time and minimum recovery time of the prepared compound samples to NO_2 gas were at an operating temperature of 300 ºC. Table (4) shows the minimum values of the response and recovery times.

Table 4: Minimum response time and recovery time of ferrite nanoparticles $Cu_xAl_{0.3-x}Ni_{0.7}Fe_2O_4$ samples to NO_2 gas.

Content (mole)	Minimum response time (sec)	Minimum recovery time (sec)
0.05	15.3	54.9
0.1	24.3	45.9
0.15	17.1	54.9
0.2	23.4	48.6
0.25	23.4	60.3
0.3	16.2	53.1

3.4. Magnetic properties

The shape and size of the magnetic hysteresis ring for each sample of the ferrite nanoparticles $Cu_xAl_{0.3-x}Ni_{0.7}Fe_2O_4$ were obtained with the Vibration Magnetic Device (VSM) (EZ VSM Model 10), as shown in Figure (6). It can be noticed that the rings of magnetic hysteresis for all the samples are small and narrow, this indicates that the wasted energy is low. When the magnetic field is absent (equal to zero), the area of the magnetic retardation curve in the material is large and wide, so the demagnetizing field (the opposite field) is large, which means that the material retains magnetism for a long time. In contrast, a narrow curve indicates a small demagnetizing field [23, 24].

The length of the magnetic hysteresis loop (magnetic hysteresis) plays an important role in the magnetic properties of the material. Small and narrow hysteresis loop means that the wasted energy is as little as possible, and it can, therefore, be used as magnetic hearts in generators. It also means that this type of material has the best magnetic properties. Soft ferrite is an alternative to the materials used previously (wrought iron sheets) in building the cores of transformers and electric generators, in addition to its widespread use in the engineering and electronic fields [25, 26].

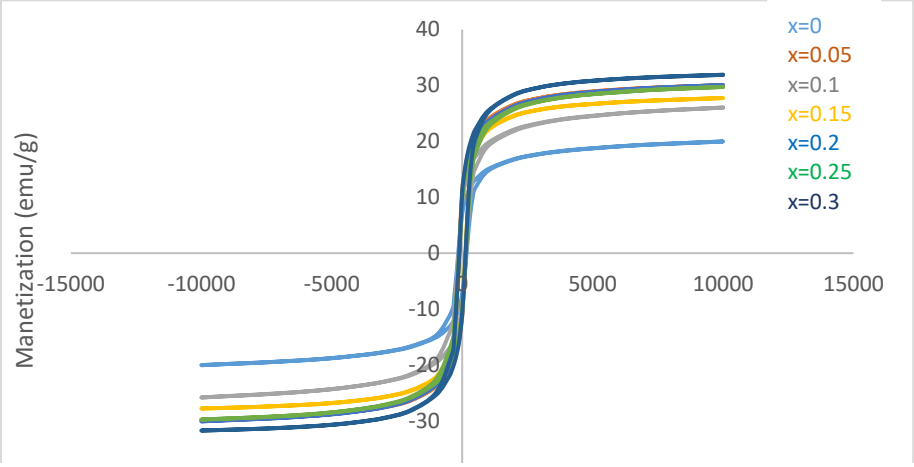

Figure 6: The relationship between magnetism of $Cu_xAl_{0.3-x}Ni_{0.7}Fe_2O_4$ nanoparticles samples and the applied field.

Conclusions

Ferrite single-phase nanoparticles, which contains nickel, aluminum, and copper ($Cu_xAl_{0.3-x}Ni_{0.7}Fe_2O_4$), (where x = 0, 0.05, 0.1, 0.15, 0.2, 0.25, and 0.3) was successfully prepared by the auto-combustion sol-gel method. XRD and FE-SEM tests proved the prepared compound was of ferrite nanoparticles of the spinel type with a multi-crystalline face-centered cubic (FCC) structure, and it is of high purity, i.e. monophasic. The crystal lattice constant increased with the increase of the molar concentrations of copper ions (x = 0, 0.05, 0.1, 0.15, 0.2, 0.25, and 0.3) which led to an increase in the specific surface area of the compound. The prepared compound samples showed a clear sensitivity to NO_2 gas at different operating temperatures. Most of the samples recorded the highest sensitivity at an operating temperature of 200 ºC, while the lowest response and lowest recovery times for all samples were at 300 ºC operating temperature.

References:

[1] A. I. Ayesh, A.A. Alyafei, R.S. Anjum, R.M. Mohamed, M.B. Abuharb, B. Salah, M. El-Muraikhi, "Production of sensitive gas sensors using CuO/SnO_2 nanoparticles," *Applied Physics A*, vol. 125, pp. 1-8, 2019.

[2] A. I. Ayesh, "Metal/metal-oxide nanoclusters for gas sensor applications," *Journal of Nanomaterials*, vol. 2016, Article ID 2359019, 2016.

[3] E. Comini, G. Faglia, G. Sberveglieri, Z. Pan, Z. L.Wang, " Stable and highly sensitive gas sensors based on semiconducting oxide nanobelts," *Applied physics letters*, vol. 81, no. 10, pp. 1869-1871, 2002.

[4] M. Gaidi, "Nanostructured SnO_2 thin films: effects of porosity and catalytic metals on gas-sensing sensitivity," *Applied Physics A*, vol. 124, no. 725, pp. 1-4, 2018.

[5] A. Jain, R. K. Baranwal, A. Bharti, Z. Vakil, C. S. Prajapati, "Study of Zn-Cu ferrite nanoparticles for LPG sensing," *The Scientific World Journal*, vol. 2013, Article ID 790359, 2013.

[6] L. Saheb, T. M. Al-Saadi, "Synthesis, Characterization, and NH_3 Sensing Properties of ($Zn_{0.7}Mn_{0.3-x}Ce_xFe_2O_4$) Nano-Ferrite," *Journal of Physics: Conference Series*, vol. 2114, no. 1, p. 012040, 2021.

[7] M. Qin, Q. Shuai, G. Wu, B. Zheng, Z. Wang, H. Wu, "Zinc ferrite composite material with controllable morphology and its applications," *Materials Science and Engineering: B*, vol. 224, no.1, pp. 125-38, 2017.

[8] O. A. Ahmed, A. H. Abed, T. M. Al-Saadi, "Magnetic Properties and Structural Analysis of Ce-Doped Mg–Cr Nano-Ferrites Synthesized Using Auto-Combustion Techniqu," *Macromolecula*

Symposia, Special Issue: International Conference on Science and Engineering of Materials ICSEM 2021 Part I, vol. 401, no. 1, p. 2100311, 2022.

[9] K. K. Bharathi, J. A. Chelvane, G. Markandeyulu, "Magnetoelectric properties of Gd and Nd-doped nickel ferrite," *Journal of Magnetism and Magnetic Materials*, vol. 321, no. 22, pp. 3677-3680, 2009.

[10] M. Tsvetkov, M. Milanova, I. Ivanova, D. Neov, Z. Cherkezova-Zheleva, J. Zaharieva, M. Abrashev, "Phase composition and crystal structure determination of cobalt ferrite, modified with Ce, Nd and Dy ions by X-ray and neutron diffraction," *Journal of Molecular Structure*, vol. 1179, no. 5, pp. 233-41, 2019.

[11] T. M. Al-Saadi, L. J. Alsaady, "Preparation of Silver Nanoparticles by Sol-Gel Method and Study their Characteristics," *Ibn Al-Haitham Journal for Pure and Applied Sciences*, vol. 28, no. 1, pp. 301-310, 2015.

[12] K. M. Musa, T. M. Al-Saadi, "Investigating the Structural and Magnetic Properties of Nickel Oxide Nanoparticles Prepared by Precipitation Method," *Ibn Al-Haitham Journal for Pure and Applied Sciences*, vol. 35, no. 4, pp. 94-103, 2022.

[13] T. M. Al-Saadi, A. H. Abed, A. A. Salih, "Synthesis and Characterization of $AlyCu_{0.15}Zn_{0.85-y}Fe_2O_4$ Ferrite Prepared by the Sol-Gel Method," *Int. J. Electrochem. Sci.*, vol. 13, pp. 8295-8302, 2018.

[14] T. M. Al-Saadi, M. A. Jihad, "Preparation of graphene flakes and studying its structural properties," *Iraqi Journal of Science*, vol. 57, no. 1, pp. 153-45, 2016.

[15] A. Kumar, Annveer, M. Arora, M. S. Yadav, R. P. Panta, "Induced size effect on Ni doped nickel zinc ferrite nanoparticles," *Physics Procedia*, vol. 9, pp. 20-23, 2010.

[16] P. P. Hankare, V. T. Vader, N. M. Patil, S. D. Jadhav, U. B. Sankpal, M. R. Kadam, B. K. Chougule, N. S. Gajbhiye, "Synthesis, characterization and studies on magnetic and electrical properties of Mg ferrite with Cr substitution," *Materials Chemistry and Physics*, vol. 113, no. 1, pp. 233-238, 2009.

[17] B. P. Jacob, S. Thankachan, S. Xavier, E. M. Mohammed, "Dielectric behavior and AC conductivity of Tb^{+3} doped $Ni_{0.4}Zn_{0.6}Fe_2O_4$ nanoparticles," *Journal of Alloys and Compounds*, vol. 541, no. 15, pp. 29-35, 2012.

[18] S. S. Suryawanshi, V. V. Deshpande, U. B. Deshmukh, S. M.Kabur, N. D. Chaudhari, S. R. Sawant, "XRD analysis and bulk magnetic properties of Al^{+3} substituted Cu–Cd ferrites," *Materials chemistry and physics*, vol. 59, no. 3, pp. 199-203, 1999.

[19] V. T. Vader, R. S. Pandav, S. D. Delekar, "Structural and electrical studies on sol–gel synthesized fine particles of Mg–Ni ferrichromite," *Journal of Materials Science: Materials in Electronics*, vol. 24, pp.4085-91, 2013.

[20] J. Xuan, G. Zhao, M. Sun, F. Jia, X. Wang, T. Zhou, G. Yin, B. Liu, "Low-temperature operating ZnO-based NO_2 sensors: a review," *RSC Adv.*, vol. 10, no. 65, pp. 39786-39807, 2020.

[21] K. Yahya, "Characterization of Pure and Dopant TiO_2 Thin Films for Gas Sensors Applications," Ph. D. Thesis, University of Technology Department of Applied Science. 2010.

[22] A. Yüce, B. Saruhan, "1.1. 3 Al-doped TiO_2 semiconductor gas sensor for NO_2-detection at elevated temperatures," *Tagungsband*, vol. 21, pp. 68-71, 2012.

[23] X. Liu, W. Zhong, S. Yang, Z. Yu, B. Gu, Y. Du, "Influences of La^{+3} substitution on the structure and magnetic properties of M-type strontium ferrites," *Journal of Magnetism and Magnetic Materials*, vol. 238, no. 2-3, pp. 207-214, 2002.

[24] V. Turchenko, V.G. Kostishin, S. Trukhanov, F. Damay, M. Balasoiu, B. Bozzo, I. Fina, V. V. Burkhovetsky, S. Polosan, M. V. Zdorovets, A. L. Kozlovskiy, "Structural features, magnetic and ferroelectric properties of $SrFe_{10.8}In_{1.2}O_{19}$ compound," *Materials Research Bulletin*, vol. 138, no. 1, p. 11236, 2021.

[25] M. T. Farid, I. Ahmad, M. Kanwal, G. Murtaza, I. Ali, S. A. Khan, "The role of praseodymium substituted ions on electrical and magnetic properties of Mg spinel ferrites," *Journal of Magnetism and Magnetic Materials*, vol. 428, pp. 136-43, 2017.

[26] Q. Lin, J. Lin, Y. He, R. Wang, J. Dong, "The structural and magnetic properties of gadolinium doped $CoFe_2O_4$ nanoferrites," *Journal of Nanomaterials*, vol. 2015, Article ID 294239, 2015.